

A Note on Relationships between Sea Surface Roughness and Altimeter Backscatter

B. Chapron¹, K. Katsaros¹, T. Elfouhaily¹, and D. Vandemark²

¹Département d'Océanographie Spatiale
IFREMER, BP 70, 29280 Plouzané, France

²NASA/Goddard Space Flight Center, Laboratory for Hydrospheric Processes
Wallops Island, VA 23337, USA

Abstract

We present a sea scattering model for the radar altimeter. Central to this effort is definition of an idealized omnidirectional spectrum approximation in the high-wavenumber spectral domain. This spectrum is consistent with recent forms showing two distinct energy balance regimes and is constrained to the well-known optical slope observations made by *Cox and Munk* [1954]. Scattering prediction relies on the two-scale Kirchhoff method at vertical incidence to treat the dominant quasi-specular scattering but also to permit examination of diffraction caused by high-frequency waves. Using satellite altimeter data, attention is devoted to clarifying relationships between altimeter normalized cross section σ_0 , surface wind speed, and sea surface slope and height variance. Results indicate that Ku-band backscatter for wind speeds above 7 m/s is sensitive, as expected, to changes in total surface roughness, but also to changes in the more highly wind-dependent gravity-capillary range between 2 and 10 cm. Modeled frequency dependencies related to small-scale roughness are compared to global TOPEX Ku-band and C-band altimeter data showing promising agreement. For example, the physically-based development is able to reproduce a well-defined transition between the two frequencies of TOPEX measurements, observed near 7 m/s wind speed, presumably associated with the onset of boundary layer-flow separation and wave breaking events.

1 Introduction

Microwave altimeter ocean backscatter σ_0 is fundamentally related to *sea surface roughness*. An application is found in the robust, empirically-derived wind retrieval algorithm for Ku-band (13.9 GHz) instruments [*Witter and Chelton*, 1991]. Theoretical or physically-based scattering model studies [*Barrick*, 1968; *Brown*, 1978; *Jackson et al.*, 1992; *Wu*, 1994] suggest that there is a more direct altimeter inference to be made in terms of surface *mean square slope (mss)*, which should parallel the classical optical measurements of ocean *mss* versus wind speed provided by *Cox and Munk* [1954]. Uses for global *mss* data sets in air-sea interaction research are increasingly apparent. Indeed, wind induced wave motions tend to modify gas transfer

rates which are further enhanced when the waves break entraining bubbles and producing spray. It has been observed in laboratory conditions that gas transfer velocities significantly increase at the onset of surface wave generation. Moreover, measurements seem to indicate that gas transfer enhancement correlates well with surface roughness and *mss* parameters [Coantic, 1980; Jähne *et al.*, 1987; Wanninkhof and Bliven, 1991].

Potentially, information on gas transfer is thus available from the global satellite data sets, but, is altimeter backscatter solely related to integrated surface roughness? While strict adherence to specular-point scattering theory requires that this be the case, Thompson [1988] among others, have advanced the idea that some attenuation of near-vertical backscatter can be due to diffraction effects caused by small-scale waves. The theory is that under a two-scale Gaussian approximation for the surface, the predominant backscatter will come from quasi-specular reflections due to long-scale slopes, but short-scale waves below the high-frequency (or cut-off) limit will diffract radiation in proportion to their height spectral density. Such an effect may skew the traditional filtered-surface (mean square slope) interpretation and also indicates potential for a second frequency dependency in altimeter backscatter modeling. To investigate this idea, we employ the Kirchhoff integral equation approach (also termed the correlation function approach), use of a two-scale surface approximation, and consideration of the Rayleigh parameter associated with surface roughness and carrier frequency [Jackson *et al.*, 1992]. An integral part of this development is definition of the sea surface input to the scattering model. Much effort has gone into reconciling measurement and theory regarding the functional form for the *high-frequency wave spectrum* [e.g., Apel, 1994]. Our proposed omnidirectional form is representative of recent spectra indicating two distinct energy balance regimes, the gravity-capillary regime being more strongly wind-dependent than the short-gravity range as suggested by Donelan and Pierson [1987]. This spectrum is explicitly defined to conform to Cox and Munk's [1954] slick and clean surface slope measurements.

A key motivation for this study is the global dual-frequency (C and Ku-band) altimeter data set available from the TOPEX satellite. These data, combined with a representative, empirically-derived Ku-band altimeter wind speed algorithm, provide a sound basis for evaluation of specular-point and two-scale Kirchhoff solutions, in terms of both wind-speed and transmit-frequency dependencies. We note that our goal is not to analyze individual anomalies in altimeter data which might be due, among other processes, to wind variability, atmospheric stratification, sea state or fetch effects as well as erroneous atmospheric correction and instrumental noise. We chose a global data set including a large range of situations, but we limited it to cases with low atmospheric correction to permit us to extract mean tendencies.

2 Semi-Empirical Sea Spectrum

For examination of near-vertical incidence radar altimeter returns, accounting for wind directivity is not essential. Thus, the approximation presented here is an idealized one-dimensional form in the high-frequency spectral regime. To define this spectral tail region, we follow the approach used by *Rodriguez et al.* [1992]. For our investigation, we have only modified their proposed simplified analytical spectrum in order to further incorporate recent observations and theoretical developments. The spectral peak level is linearly dependent on the wind speed, U , 10 m above the surface. Although in the along-wind direction the directional spectrum may exhibit a classical Phillips' -4 power law dependence over the entire gravity wave range [*Banner et al.*, 1989], slope of the nondirectional spectrum is chosen to follow a -2.5 power law dependence for wavenumber greater than the peak and smaller than about 10 times the spectral peak wavenumber. Such a form follows *Kitaigorodski's* [1983] theoretical arguments and the Donelan and Pierson spectrum model. The peak spectral wavenumber is approximately given by g/U^2 , where g is the acceleration of gravity. To insure reasonable mean square slope estimates, we constrain the spectrum so we obtain the optical slope estimates of wind roughened natural clean and artificial slick sea surfaces made by *Cox and Munk* [1954]. For the slick surface, wave components shorter than a foot were almost absent, so a partial integration of our slope spectrum between the peak wavelength and 30 cm wavelength yield that result. For the clean surface, all wave components must contribute to the total mean square slope. The Cox and Munk clean and slick relationships are respectively [*Phillips*, 1977; *Wu*, 1990]:

$$m_{SS_{clean}} = .003 + 5.12 \times 10^{-3}U \quad m_{SS_{slick}} = .0046 \log(k_{slick}U^2/g) \quad (1)$$

where $k_{slick} = 2\pi/.3$ rad/m. In the high wavenumber pure capillary region, rapid decay, due mainly to viscous dissipation, is required so that contributions of millimeter waves can be ignored. Following recent *in situ* and laboratory optical measurements [*Klinke and Jähne*, 1994; *Hara et al.*, 1994], we set a secondary higher-wavenumber peak just before this fast decay. The analytical form of our spectral model for $U > 7$ m/s is then

$$F(k) = k^{-2.5} \times (s_1 e^{-k/k_1} + s_2 e^{-(k/k_2)^2}) \quad (2)$$

for $k > k_0 = g/U^2$ rad/m, and where $k_1 = 2\pi/.21 \times e^{-U/4.9}$ rad/m and $k_2 = 365$ rad/m. The spectral coefficients s_1 and s_2 are computed so the spectrum simultaneously satisfies (1) and a final condition

$$F(k_0) = 2.25 \times 10^{-3} \frac{U}{g^{1/2}} k_0^{-2.5} \quad (3)$$

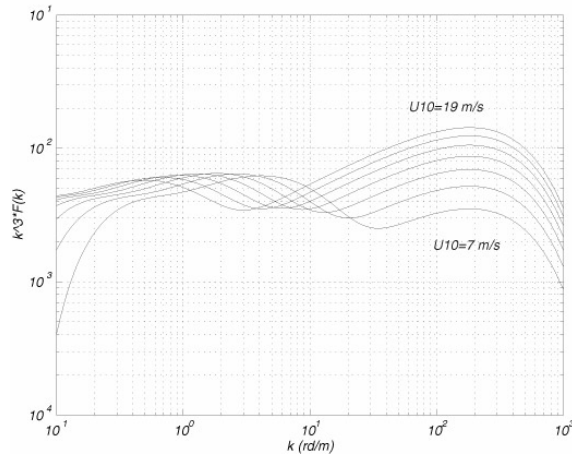


Figure 1: Omnidirectional saturation spectra for several wind speeds

to match data presented by Khama [Khama, 1981]. Figure 1 shows omnidirectional saturation spectra for several wind speeds ranging from 7 m/s to 19 m/s with a step of 2 m/s. A feature of this spectrum is that the *mss* computation can be analytically carried out to permit derivation of the constants, s_1 and s_2 .

3 A Two-Scale Scattering Model

The general problem of electromagnetic scattering from the rough sea surface can be approached in a variety of ways. Among them, Geometrical Optics (GO) (or specular-point) formulations have been proposed to describe ocean surface returns for small incidence angles. GO prediction works in the high-frequency limit, that is when surface roughness is large compared with the incident radiation wavelength, λ_i . Backscatter is treated as the incoherent addition of quasi-specular reflections from specular points associated with facets with dimensions $\geq 3\lambda_i$ [Brown, 1978]. Scattering from roughness scales below this dimension violates the theory's limitation. The GO solutions offers a simple, physically-intuitive expression relating the intensity of the return radiation in terms of joint *pdf* of surface height and specular slope. For Gaussian surface statistics and normal incidence, the GO approximation reduces to $\sigma_0 \propto 1./mss_{GO}$. mss_{GO} is the filtered mean square slope defined under GO theory, to differentiate between total *mss* and the partial *mss* available to the microwave altimeter because it cannot derive slope variance from waves of length below $3\lambda_i$. Ignoring wave directionality because of the normal incidence, this filtered slope variance is computed from our spectral model, as

$$mss_{GO} = \int_{k_{peak}}^{k_{cut}} F(k)k^2 dk \quad (4)$$

where $k_{cut} = 2\pi/(3\lambda_i)$ is the cut-off wavenumber eliminating short-scale waves from the integration.

As a recognized alternative, the Physical Optics (PO) or Kirchhoff integral solution for the far-zone backscatter cross-section of a perfectly conducting Gaussian random isotropic rough surface can be written as

$$\sigma_0 = 2k_i^2 \int e^{-4k_i^2(\rho(0)-\rho(r))} r dr \quad (5)$$

with $k_i = 2\pi/\lambda_i$ incident radar wavenumber and ρ is the surface correlation function. Assuming perfect conductivity and the absence of shadowing effects, the PO solution reduces to the GO solution in the high-frequency limit [Brown, 1990]. However, the PO form will permit 'violation' of this limit. A frequently-cited approximation for the PO solution assumes that the surface can be spectrally decomposed into statistically independent large and small scale components. Such a decomposition is possible under Gaussian statistical description, and the correlation function can be written as $\rho(r) = \rho_L(r) + \rho_s(r)$. The break between scales is set by the high-frequency scattering limit to be k_{cut} . To simplify the large-scale contribution, one can expand the large-scale correlation function (Taylor series) and neglect the curvature (quartic) terms, leaving the parabolic second order terms containing the mean square slope. Expression (5) becomes

$$\sigma_0 = 2k_i^2 e^{-4k_i^2 \rho_s(0)} \int e^{-k_i^2 mss_{GO} r^2} e^{4k_i^2 \rho_s(r)} r dr \quad (6)$$

In this expression, explicit accounting for diffraction effects is carried by the exponential term in front the integral. If the Rayleigh parameter, $k_i \sqrt{\rho_s(0)}$, becomes non-negligible, attenuation of radar cross section is predicted. Otherwise, (6) reduces to the GO solution.

This *two-scale Kirchhoff solution* is known [Thompson, 1988] and is analogous to two-scale scattering at moderate incidence angles. At those angles, diffraction dominates but specular contributions are added in the *ad hoc* two-scale methodology. That composite prediction was suggested to bring prediction in line with observations. As with scatterometry, we suggest that a 'violation', in this case, of the high-frequency scattering limit, appears justified when comparing data and model. The difference between GO and PO solutions in interpreting σ_0 versus wind speed is clear when examining figure 1 and considering the Ku-band microwave altimeter cut-off wavenumber of 100 rad/m. One can see that while slope in the large scale regime $< k_{cut}$

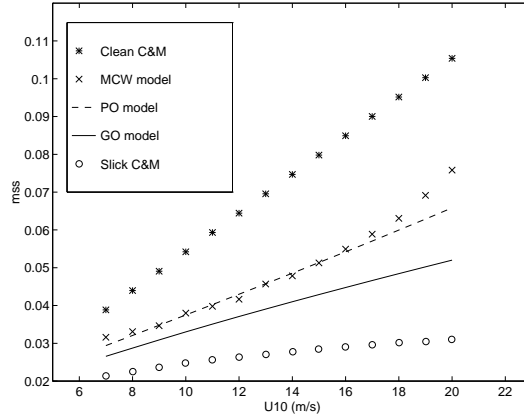


Figure 2: Mean square slope parameter versus wind speed U_{10}

increases, there is also a strong wind-dependence in the region above the cut-off (8–2 cm) gravity-capillary waves. This is borne out by scatterometer observations where the radar Bragg wavenumbers were at these short scales. In (6), the Rayleigh parameter will be quite small for Ku-band, but not negligible. Values should range from near 0 at 7 m/s to 0.4 at 20 m/s. At C-band, k_i is nearly three times smaller while small-scale height density changes little, therefore a C-band altimeter should be much less sensitive to wind changes entering into (6) through diffraction effects. Thus, the result of (6) is that while a C- and Ku-band altimeter should respond similarly to changes in large-scale slope variance, providing an almost redundant estimate, there will be additional, diffraction-caused attenuation evident in the Ku-band signal as wind increases. At this stage we note that we concentrate on $U > 7$ m/s for the reason that wind influence on the surface is better-understood above this level. Below this wind speed, both scattering and wind-wave theory require more attention than we can give here.

One test of a physically-based altimeter model should be its ability to reproduce observations and operational algorithms. Here, we consider the Modified Chelton-Wentz (MCW) operational wind speed retrieval algorithm [Witter and Chelton, 1991] for the Ku-band altimeter. To compare model results, figure 2 shows predictions as U_{10} against mss , where we define mss for the two-scale PO model (6) and MCW as $\propto 1./\sigma_0$ and mss_{GO} from (4). The spectral model of section 2 is used for GO and PO computations. The agreement between the model (7) and MCW is quite good, and is clearly better than the specular model. As discussed above, the added attenuation (seen here as increased mss) from the small-scale diffraction component of (7) is evident in comparing mss_{PO} to mss_{GO} . Increasing divergence between full integral model and filtered surface slope variances is interpreted as an increasing wind influence on small wave spectral density development.

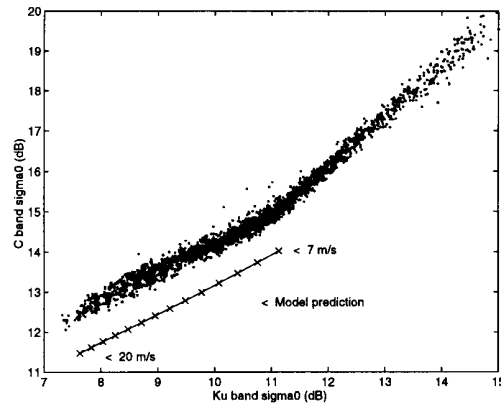


Figure 3: Predicted model results and global data

4 TOPEX Dual-Frequency Measurements

In the preceding section, we used the Kirchhoff model (6) in conjunction with an idealized short scale wave spectrum to predict wind dependent Ku-band altimeter returns. Results were close, particularly in form, to those predicted by the MCW operational empirical algorithm. The same physically-based model can be used to predict wind dependent C-band altimeter returns. Results can then be compared against a global C- and Ku-band data set from the TOPEX mission. Because absolute calibration information for C-band TOPEX data is unavailable, we will look at these comparisons in a relative manner. Selected TOPEX data correspond to a small subset of cycle 70 (10 orbits) acquired over deep-ocean areas. This cycle was chosen for its overall gain stability. Ku-band σ_0 data have been shifted (in dB) according to AVISO [1995]. Figure 3 presents predicted model results and data. Aside from a shift along the C-band axis (dB), our physically-based development reproduces the relationship between dual-frequency TOPEX measurements for even the lowest measured σ_0 (highest sea surface roughened case). A least-square adjustment between model prediction and data gives an *ad hoc* calibration constant for the TOPEX C-band data of about -1 dB.

Using this C-band calibration, figure 4 shows inferred altimeter and model results. Overall good agreement is clearly obtained for the highest *mss* parameters. This graph clearly reveals change in sensitivity between C- and Ku-band as sea surface roughness increases. However, C-band measurements do not dramatically saturate at high wind speed as would have been predicted by using the MCW algorithm to invert Ku-band data. The change in sensitivity occurs near 7 m/s wind speed. Such a transition may be associated with the transition from aerodynamically smooth to rough flow with onset of increased small scale wave breaking events [Banner and Melville,

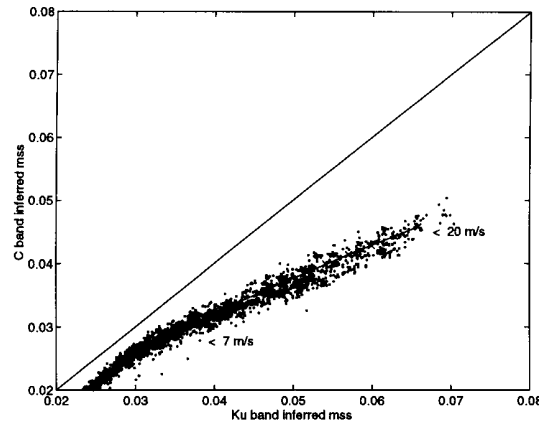


Figure 4: Inferred altimeter mean square slope parameter and model results

1976]. According to the scattering model development and the proposed idealized spectrum, increasing departure between C- and Ku-band data in the higher wind regime can be directly associated with increase in the integrated roughness but also, with changes in the more highly wind dependent gravity-capillary range between 2 and 10 cm waves. This is consistent with *in situ* and laboratory high resolution optical measurement as well as with the Donelan-Pierson spectral form in this range.

5 Summary

A *two-scale Kirchhoff scattering model* for the altimeter appears to provide a more consistent physical interpretation of satellite σ_0 data than a strict specular-point, or filtered-surface approach. A brief discussion of the model and implications indicate that, while the predominant altimeter backscatter is derived from large-scale slope variance, significant attenuation of the Ku-band signal can be attributed to diffraction effects of surface ripples below the large-scale cut-off wavelength. This was demonstrated with model comparison to the MCW wind speed retrieval algorithm. The effect of *small-scale wave growth* appears above about 7 m/s and is quantitatively derived based on the input wave spectral model provided in Section 2. This idealized wave model is in agreement with recent theory and optical measurements, particularly regarding high-wavenumber characteristics. The present development represents a first-order use of scattering theory and surface description that, while brief and incomplete in several aspects, points out important distinctions between optically-derived total *mss* and what the vertically-pointed microwave altimeter should be used to infer. The spectral model and integral equation approach are presently being tested for self-consistency through

comparisons against scatterometer algorithms and data sets.

Simultaneous dual-frequency TOPEX σ_0 data demonstrate the potential to go beyond empirical wind speed relationships. We observe that C- and Ku-band backscatter measurements show a large departure in the form of the wind-dependence function starting at about 7 m/s, a change, too abrupt to predict using a filtered-surface slope model and realistic wave spectrum. Even though the Ku-band model comparison with MCW in figure 3 suggests the growth of small-scale waves beyond this wind speed, the dual-frequency TOPEX data present an example where a two channel altimeter can clarify the picture considerably better. The observed data, interpreted using the Kirchhoff model, suggest a marker for the onset of small-scale wave growth, apparent in the Ku-band channel ($\lambda = 2.1$ cm) but not yet apparent at that wind speed for C-band ($\lambda = 5.5$ cm). We stress that we used global data, thus potentially indicating a fundamental change in the surface-roughness-to-wind relation near 7 m/s. Beyond this critical wind speed, it is known that generation of small-scale wind waves is responsible for a significant fraction of the mean sea surface wind stress [Makin et al., 1995]. TOPEX data and the present scattering model should aid attempts to refine definitions of ultra-high wavenumber spectral densities.

In conclusion, acknowledging that an altimeter's areal coverage and non-directionality limit its contribution to wind field mapping, it is nevertheless clear that from a climatic standpoint global altimeter backscatter data are valuable. Defining momentum transfer to the ocean surface is a critical component in air/sea coupled modeling with inferences for both heat and gas transfer. A multiple (3 or 4) frequency altimeter could possibly allow differentiation between surface roughness changes among wavenumbers in the high-frequency wave regime (eg. $2 \text{ cm} > \lambda > 300 \text{ cm}$) for relating various air/sea processes. These waves seem to support most of the momentum transfer [Caudal, 1993]. Other scales may dominate heat and gas transfer, and such a multiple frequency instrument would help to better clarify a number of processes occurring at the interface contributing to these different transfers.

References

- Apel, J. R., An improved model of the ocean surface wave vector spectrum and its effect on radar backscatter, *J. Geophys. Res.*, 99, 16269–16291, 1994
- AVISO, AVISO CD ROM user guide: merged GDR status (cycles 1 to 90), *AVI-NT-02-102-CN*, 1995
- Banner, M. L., I. S. F. Jones and J. C. Trinder, Wavenumber spectra of short gravity waves, *J. Fluid Mech.*, 198, 321–344, 1989
- Banner, M. L. and W. K. Melville, On the separation of air-flow over water waves, *J. Fluid Mech.*, 77, 825–842, 1976
- Brown, G. S., Backscattering from a Gaussian distributed, perfectly conducting, rough surface, *IEEE trans. Anten. Propag.*, AP-26, 472–482, 1978

- Brown, G. S., Quasi-specular scattering from the air-sea interface, *Surface waves and fluxes*, Vol. II, Geernaert and Plant editors, 1-40, 1990
- Caudal G., Self-consistency between wind stress, wave spectrum and wind-induced wave growth for fully rough air-sea interface, *J. Geophys. Res.*, 98, 22743, 1993
- Coantic, M., Mass transfer across the ocean/air interface: small scale hydrodynamic and aerodynamic mechanisms, *Physicochemical Hydro.*, 1, 249-279, 1980
- Cox C. S., and W. H. Munk, Measurements of the roughness of the sea surface from photographs of the sun's glitter, *J. Opt. Soc. Am.*, 44, 838, 1954
- Donelan M. A., and W. J. P. Pierson, Radar scattering and equilibrium ranges in wind-generated waves with application to scatterometry, *J. Geophys. Res.*, 92, 4971, 1987
- Hara, T., E. J. Bock and D. Lyzenga, In situ measurements of capillary-gravity wave spectra using a scanning laser slope gauge and microwave radar, *J. Geophys. Res.*, 99, 12593, 1994
- Jackson, F. C., W. T. Walton and D. E. Hines, Sea surface mean square slope from Ku-band backscatter data, *J. Geophys. Res.*, 97, 11411-11427, 1992
- Jähne, B., K. O. Münnich, R. Börsinger, A. Dutzi, W. Huber and P. Libner, On the parameters influencing air-water gas-exchange, *J. Geophys. Res.*, 92, 1937-1949, 1987
- Jähne, B. and K. Riemer, Two-dimensional wave number spectra of small-scale water surface waves, *J. Geophys. Res.*, 95, 11531-11546, 1990.
- Khama, K. K., A study of the growth of the wave spectrum with fetch, *J. Phys. Oceanogr.*, 11, 1503-1515, 1981
- Kitaigorodski, S. A., On the theory of the equilibrium range in the spectrum of wind-generated gravity waves, *J. Phys. Oceanogr.*, 13, 816-827, 1983
- Klinke J. and B. Jähne, Measurements of small-scale structure of the ocean surface with new optical instrument, Preprints of 2nd Intl. Conf. on Air-Sea Interaction and on Meteorology and Oceanography of the Coastal Zone, *Amer. Met. Soc.*, 102-103, 1994
- Makin, V. K., V. N. Kudryavtsev and C. Mastenbroek, Drag of the sea surface, *Bound.-Layer Meteo.*, 73, 159-182, 1995
- Phillips, O. M., The dynamics of the upper ocean, *Cambridge University Press*, 1977
- Rodriguez, E., Y. Kim and J. M. Martin, The effect of small-wave modulation on the electromagnetic bias, *J. Geophys. Res.*, 97, 2379-2389, 1992
- Thompson, D. R., Calculation of radar backscatter modulations from internal waves, *J. Geophys. Res.*, 93, 12371-12380, 1988
- Witter, D. L., and D. B. Chelton, A GEOSAT altimeter wind speed algorithm and a method for altimeter wind speed algorithm development, *J. Geophys. Res.*, 96, 8853, 1991
- Wanninkhof, R.H., and L. F. Bliven, Relationship between gas exchange, wind speed, and radar backscatter in a large wind-wave tank, *JGR* 96, 2785-2796, 1991.
- Wu, J., Mean square slopes of the wind-disturbed water surface, their magnitude, directionality and composition, *Radio Science*, 25, 37-48, 1990
- Wu, J., Microwave specular reflections from sea surface-A continuous altimeter-wind algorithm from breeze to hurricane, Preprints of 2nd Intl. Conf. on Air-Sea Interaction and on Meteorology and Oceanography of the Coastal Zone, *Amer. Met. Soc.*, 276-277, 1994